Available online at www.sciencedirect.com
SCIENCE DIRECT®
Journal of Sound and Vibration 277 (2004) 405–418
JOURNAL OF SOUND AND VIBRATION
www.elsevier.com/locate/jsvi

Letter to the Editor

# On the influence of boundary constraints and angled baffle arrangements on sound radiation from rectangular plates ☆

M. Ohlrich[a,*], C.T. Hugin[b,1]

[a] *Ørsted-DTU, Acoustic Technology, Technical University of Denmark, Building 352, DK-2800 Kgs. Lyngby, Denmark*
[b] *ESDU International plc, 27 Corsham Street, London N1 6UA, UK*

Received 15 August 2003; accepted 17 November 2003

## 1. Introduction

Predictions of high frequency interior noise levels in transportation vehicles and aircraft structures are normally based on Statistical Energy Analysis [1]. An important parameter in such models is the coupling loss factor that describes the exchange of power between the vibrating panel structures and the acoustic cavity formed by the cabin. This coupling loss factor is often calculated from knowledge of the radiation efficiency, which describes the relation between the mean-square vibration velocity (time and spatially averaged) of the structure and the sound power it radiates into a semi-infinite fluid space. Expressions for a modal-averaged radiation efficiency of a simply supported, rectangular isotropic plate placed in an otherwise rigid co-planar baffle were first derived by Maidanik [2]. Leppington et al. [3] have given a more detailed analysis of this particular case together with an improved expression for the modal-averaged radiation efficiency at the coincidence frequency. In practice, the conditions of simply supported edges and a plane baffle are rarely fulfilled. These two factors have been known to have a non-negligible influence on the radiation efficiency below the coincidence frequency, see for example Heron [4] and Fahy [5]. More recently, expressions have been derived that permit calculation of the radiation efficiency of plates having constraint conditions at the edges that are somewhere between simply supported and clamped [6], and further with a baffle that is not necessarily co-planar with the plate, but has an arbitrary wedge-shaped form [7].

In this paper the analytical results of Leppington et al. [3,6,7] are employed in two ways. Firstly, for isotropic plates, they are used to calculate modal-averaged correction factors that allow the

☆ This is a modified version of a paper presented at the International Conference on Noise & Vibration Pre-design and Characterisation using Energy Methods (NOVEM 2000), 31 August–2 September 2000, Lyon, France.

*Corresponding author. Fax: +45-458-805-77.
*E-mail address:* mo@oersted.dtu.dk (M. Ohlrich).
[1] Now with QinetiQ, Cody Technology Park, Room 1001, Glauert Building (A9), Farnborough, Hampshire GU14 0LX, UK.

0022-460X/$ - see front matter © 2004 Elsevier Ltd. All rights reserved.
doi:10.1016/j.jsv.2003.11.038

modal-averaged radiation efficiency of edge modes to be corrected for the influence of the boundary constraint conditions as well as the angle of the baffle. Secondly, the asymptotic and transition expressions for the radiation efficiency are used in a numerical routine to calculate modal-averaged radiation efficiencies for orthotropic plates. Finally, radiation efficiencies of a practically mounted isotropic plate are predicted and validated experimentally for three typical baffle angles, namely $\pi/2$, $\pi$ and $3\pi/2$ radians. These baffle angles correspond to practical arrangements where the plate radiates, respectively, (i) into a rigid, rectangular tunnel-space or duct, (ii) into the commonly examined semi-infinite space and (iii) into a duct-excluded 'full', infinite space. The test-plate is bolted to the edges of a four-sided open box structure, which is then mounted in a fixture in order to form the various baffle configurations. The actual edge constraints describing the plate boundary conditions are estimated from measured resonance frequencies and their corresponding deformation shapes or 'mode numbers' of the plate. Predicted values of the modal-averaged radiation efficiency corrected for the influence of baffle angle and the edge constraint are compared with measured values with good agreement.

## 2. Modal-averaged sound radiation from isotropic and orthotropic plates

The radiating structure considered herein consists of a flat rectangular plate in flexural vibration. The plate has the length $a$ and width $b$ and is placed in an otherwise rigid, wedge-shaped baffle with sides that are arranged at an angle $\varphi$ relative to the $xy$-plane of the plate. This arrangement is depicted in Fig. 1, which also indicates that the plate is vibrating in a specific $r$th normal mode of vibration. This $r$th mode is characterized by the discrete bending wavenumber vector $k_r$ with wavenumber components $k_{r,x}$ and $k_{r,y}$ in the $x$ and $y$ directions, respectively, such that $k_r^2 = k_{r,x}^2 + k_{r,y}^2$. In the plane of the plate the inclination angle $\theta_r$ of the wavenumber vector $k_r$

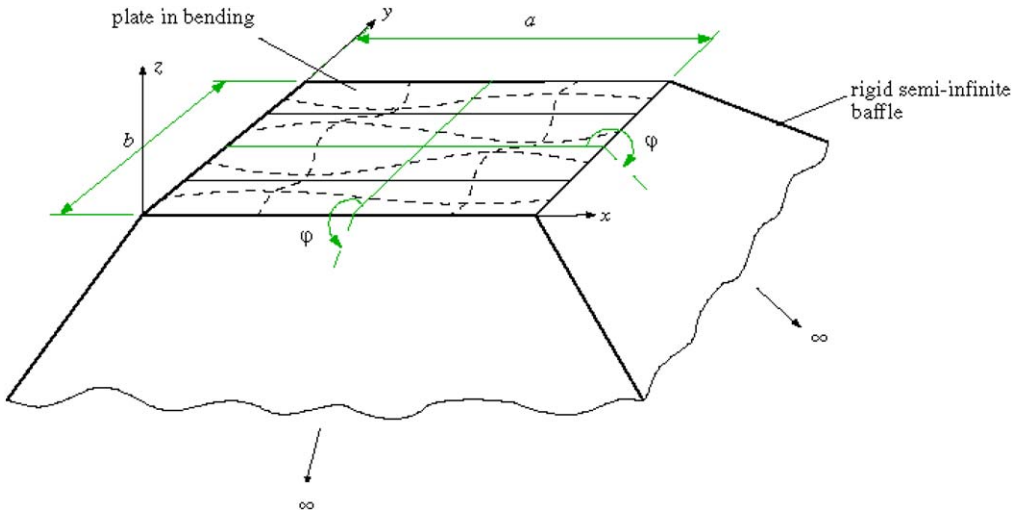


Fig. 1. Vibrating rectangular plate placed in a wedge-shaped, rigid baffle.

with respect to the $x$-axis thus reads $\theta_r = \arctan(k_{r,y}/k_{r,x})$. Therefore, the normal mode can be considered as the result of to and fro 'bouncing' plane waves with inclination $\theta_r$ and wavenumber $k_r$. Although $k_r$ and hence $\theta_r$ take discrete values accordingly, it was found [3] that it is mathematically convenient in radiation predictions to consider the plate's free bending wavenumber vector $k_b \equiv k_r$ and the inclination angle $\theta \equiv \theta_r$ to vary continuously over all relevant values.

### 2.1. Isotropic plates

The sound radiation efficiency $\sigma$ of a flat, isotropic plate in harmonic bending motion is known to be a function of the magnitudes of the plate's modal wavenumber-components relative to the wavenumber $k_0 = \omega/c_0$ of the acoustic medium, where $c_0$ is its speed of sound and $\omega$ is the angular frequency. This dependency is conveniently expressed by the non-dimensional parameters $\alpha$ and $\beta$ that specify the bending wavenumber components in $x$ and $y$ relative to $k_0$, as

$$\alpha = \frac{k_b \cos(\theta)}{k_0} \quad \text{and} \quad \beta = \frac{k_b \sin(\theta)}{k_0}, \tag{1,2}$$

in which the bending wavenumber is given by $k_b = (\omega^2 \rho h/D)^{1/4}$, where $\rho$ is plate density, $h$ is thickness and $D$ is the bending stiffness. It is seen that these parameters are defined in terms of the plate wavenumber vector $k_b$ and its angle of inclination $\theta$ with the $x$-axis, or in other words, the 'angle of propagation' of bending waves.

Leppington et al. [3] have developed asymptotic expressions for the radiation efficiency of a *simply supported* plate set in a rigid, co-planar baffle. His modal representation of the radiation efficiency will be denoted by $\sigma_{ss}(\omega, \alpha, \beta) = \sigma_{ss}(\theta)$, and for ease of reference, some of the results for various regimes in the $(\alpha, \beta)$-representation will be given. The most important characteristic frequency for sound radiation is the coincidence frequency $\omega_c$, defined by the coincidence of plate bending phase speed with the phase speed in the acoustic medium. This angular frequency is given by $\omega_c = c_0^2(\rho h/D)^{1/2}$.

Beginning *above* the coincidence frequency, $\omega > \omega_c$, where the plate radiates as a whole, the radiation efficiency is found to be

$$\sigma_{ss}(\theta) \approx 1 \Big/ \sqrt{1 - \alpha^2 - \beta^2} \quad \text{for } \alpha^2 + \beta^2 < 1. \tag{3}$$

In the frequency range lying *below* the coincidence frequency the sound radiation is mainly dominated by plate-edge radiation (edge modes) and the radiation efficiency of the plate is found as

$$\sigma_{ss}(\theta) \approx \frac{1}{k_0 a \alpha} \frac{1}{\sqrt{\alpha^2 + \beta^2 - 1}} \left\{ 1 + \frac{\alpha^2}{\alpha^2 + \beta^2 - 1} \right\} \quad \text{for } \alpha > 1, \ \beta > 1. \tag{4}$$

A corresponding expression for the case of $\alpha < 1$, $\beta > 1$, is obtained by replacing $\alpha$ with $\beta$ and $a$ with $b$. Radiation by so-called corner modes is very small, that is

$$\sigma_{ss}(\theta) \approx 0 + O(k_0^{-2}) \quad \text{for } \alpha > 1 \wedge \beta > 1. \tag{5}$$

In addition, in Ref. [3], expressions are given for the transition zones between Eqs. (3) and (5). For example, at coincidence the radiation efficiency is found to be

$$\sigma_{ss}(\theta) = \frac{2}{15}\left\{5 - \frac{a\beta}{b\alpha}\right\}\sqrt{\frac{k_0 a}{\pi\beta}} \quad \text{for} \quad \alpha^2 + \beta^2 = 1 \wedge a\beta > b\alpha. \tag{6}$$

These expressions describe the radiation efficiency $\sigma_{ss}$ in the $(\alpha, \beta)$-domain. Fig. 2 shows an example of such a three-dimensional diagram of $\sigma_{ss}$. Coincidence corresponds to the circle ridge given by: $\alpha^2 + \beta^2 = 1$. The data-values used for calculation of Fig. 2 are for an isotropic plate with a coincidence frequency at 4000 Hz. The frequency range shown is from 1000 Hz $(\alpha, \beta = 2, 2)$ to infinity, which corresponds to $\alpha, \beta = 0, 0$.

The main difficulty with using the presented asymptotic expressions for $\sigma_{ss}$ is to determine suitable limits for when to change/switch from the asymptotic expressions to the transition expressions and vice versa. However, once such suitable limits have been determined, then the $(\alpha, \beta)$-representation of the radiation efficiency $\sigma(\theta)$ permits calculation of the very useful modal-averaged radiation efficiency $\bar{\sigma}$. This is calculated by averaging over a given frequency band $\Delta\omega$, which, in the $(\alpha, \beta)$-representation of $\sigma$, corresponds to a wavenumber band $\Delta k$ having the shape of a circle for isotropic plates. Thus, the modal-averaged radiation efficiency $\bar{\sigma}$ for an isotropic plate is calculated as

$$\bar{\sigma} = \frac{2}{\pi}\int_0^{\pi/2} \sigma(\theta)\,\mathrm{d}\theta. \tag{7}$$

From this, analytical expressions can be derived for the modal-averaged radiation efficiency $\bar{\sigma}_{ss}$ for a simply supported plate in a plane baffle, when the contribution from the insignificant corner

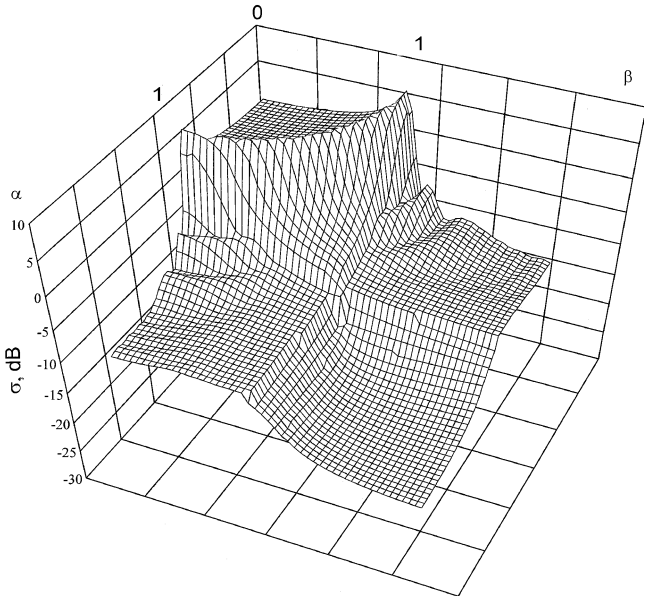


Fig. 2. Radiation efficiency, $10\log\sigma_{ss}$, for a simply supported, isotropic plate with a coincidence frequency at 4000 Hz.

region, $\alpha > 1$ and $\beta > 1$, is set to zero. This procedure leads to the same analytical expressions for $\bar{\sigma}_{ss}$ as were given in Ref. [2,3].

### 2.2. Orthotropic plates

For an orthotropic plate there are two factors that will influence the calculation of the modal-averaged radiation efficiency. Firstly, the bending wavenumber is a function of the angle $\theta$, and the integration path in the $(\alpha, \beta)$-representation of the radiation efficiency will have a shape resembling an ellipse [5]. Integration can thereby include both supersonic and subsonic bending wavenumber components. Secondly, the modal density is also a function of the angle $\theta$ and it is necessary to take this into account if the SEA requirement of equipartition of modal energy is to be fulfilled.

#### 2.2.1. Dispersion relation for the bending wavenumber

For orthotropic plates, the bending wavenumber depends upon the angle $\theta$. This dependency can be determined by considering the wave equation for thin orthotropic plates [8]

$$\frac{h^3}{12}\left\{\frac{E_x}{(1-\nu_{xy}\nu_{yx})}\frac{\partial^4 w}{\partial x^4} + 2\left\{\frac{\nu_{xy}E_y}{(1-\nu_{xy}\nu_{yx})} + 2G\right\}\frac{\partial^4 w}{\partial x^2 \partial y^2} + \frac{E_y}{(1-\nu_{xy}\nu_{yx})}\frac{\partial^4 w}{\partial y^4}\right\} + \rho h \frac{\partial^2 w}{\partial t^2} = 0, \tag{8}$$

in which $w$ is the transverse displacement of the plate, $h$ is the thickness, $\rho$ is the mass density, $E_x$ and $E_y$ are Young's modulae in the $x$ and $y$-directions, respectively, $G$ is the shear modulus and $\nu_{xy}$ and $\nu_{yx}$ are the Poisson ratios related by $E_x\nu_{yx} = E_y\nu_{xy}$.

If the displacement of the bending waves is assumed to be of the form

$$w(x, y, t) = A \exp\{-\mathrm{j}k_b \cos(\theta)x - \mathrm{j}k_b \sin(\theta)y + \mathrm{j}\omega t\}, \tag{9}$$

then substitution of Eq. (9) in Eq. (8) yields the dispersion relation for the angle-dependent bending wavenumber $k_b(\theta)$

$$k_b(\theta) = \sqrt{\omega}\sqrt[4]{\frac{\rho h}{D(\theta)}}, \tag{10}$$

where the bending stiffness $D(\theta)$, is given as

$$D(\theta) = \frac{h^3}{12}\left\{\frac{E_x \cos^4(\theta)}{(1-\nu_{xy}\nu_{yx})} + 2\left(\frac{\nu_{xy}E_y}{(1-\nu_{yx}\nu_{xy})} + 2G\right)\cos^2(\theta)\sin^2(\theta) + \frac{E_y \sin^4(\theta)}{(1-\nu_{yx}\nu_{xy})}\right\}. \tag{11}$$

The resulting wavenumber diagram given by Eqs. (10) and (11) will have a shape resembling an ellipse.

#### 2.2.2. Equipartition of modal energy

For an SEA subsystem like the bending wave field in the plate it is assumed that the total energy is evenly distributed amongst the resonant modes of the subsystem. The implication of such equipartition of modal energy for an orthotropic subsystem can be resolved by introducing

an angle-dependent modal density term $n(\theta)$, such that the subsystem modal density $n$ is determined as

$$n = \int_0^{\pi} n(\theta)\,\mathrm{d}\theta, \tag{12}$$

see, for example, Lyon et al. [1] and Langley [9]. The term $n(\theta)$, which is interpreted as the modal density (per radian) associated with waves of heading angle $\theta$, is given as

$$n(\theta) = \frac{ab}{2\pi^2} k_b(\theta) \frac{\partial k_b(\theta)}{\partial \omega}, \tag{13}$$

where the derivative expression is noted to be the (group speed)$^{-1}$ of plate waves of heading angle $\theta$. By utilizing this angle dependency the energy density of waves of heading $\theta$ in the subsystem can then be calculated as

$$e(\theta) = \frac{En(\theta)}{abn}, \tag{14}$$

where $E$ is the total energy of the subsystem of area $ab$.

Finally, the modal-averaged sound radiation efficiency $\bar{\sigma}$ for an orthotropic plate can then be calculated from the similarly modal-density-weighted expression

$$\bar{\sigma} \approx \int_0^{\pi} \frac{\sigma(\theta) n(\theta)}{n}\,\mathrm{d}\theta, \tag{15}$$

where the integration for fixed $\omega$ is performed along the path specified by Eqs. (10) and (11). It is necessary to do the integration over $\pi$, as the main axis of a general orthotropic plate might not coincide with the plate edges.

*2.2.3. Example of sound radiation from orthotropic plates in a coplanar baffle*

An example of computed results based on Eq. (15) is shown in Fig. 3; the orthotropic plate is simply supported and set in a coplanar baffle. Here, the modal-averaged radiation efficiency is calculated for a conceptual fibre-reinforced polyester plate with various values of the reinforcing ratio $E_x/E_y$, where $E_x$ and $E_y$ are Young's modulae in the $x$ and $y$ -directions, respectively. Thus, a ratio of unity corresponds to an isotropic plate while other ratios correspond to orthotropic plates of increasing degree. The base material's properties are: $E_y = 4.5 \times 10^9$ N/m$^2$; $\rho = 1250$ kg/m$^3$; $G = 1.73\ 10^9$ N/m$^2$; $v_{xy} = 0.3$; $a = 2$ m; $b = 1$ m; and $h = 0.008$ m. Note that the mass density of the plate is assumed unchanged for simplicity.

The orthotropic plates are seen to have two coincidence frequencies, $f_{c,x}$ and $f_{c,y}$, where $f_{c,x} < f_{c,y}$. Moreover, increasing values of the ratio $E_x/E_y$ results in higher radiation below $f_{c,x}$. Above $f_{c,x}$, the radiation efficiency is seen to decrease slightly with increasing values of the ratio $E_x/E_y$. Thus, as the contribution of subsonic modes increase, more of the modes lie outside the circle $\alpha^2 + \beta^2 = 1$.

## 3. Corrections for baffle angle and plate-edge constraints

The angle of the baffle as well as the plate's boundary constraint conditions will influence the radiation efficiency below the coincidence frequency. Analytical expressions have been derived in

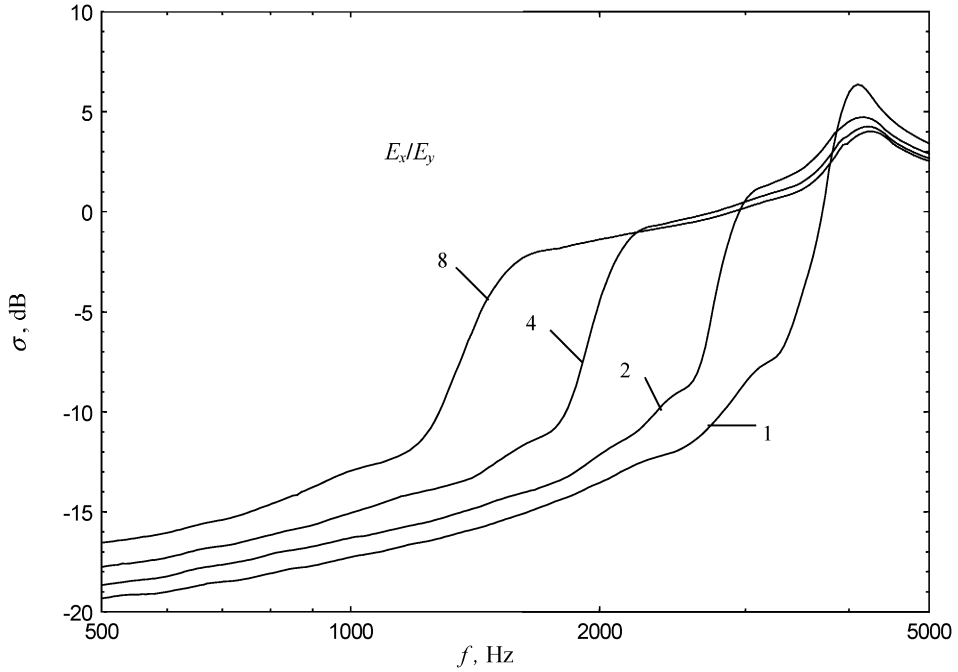


Fig. 3. Modal-averaged radiation efficiencies 10 log $\bar{\sigma}$ of a plate with various ratios $E_x/E_y$ of $x$- and $y$-wise Young's moduli.

Ref. [6] that give the radiation efficiency for edge modes when the boundary condition can be described as hinged (simply supported) with an rotational line-spring that resists the rotation of the plate edge. Hence, by changing the compliance $\varepsilon$ of the spring, the plate's boundary conditions can be varied from a rigidly clamped edge ($\varepsilon = 0$) to a simply supported edge ($\varepsilon \to \infty$). In Ref. [7], the influence of the baffle angle has been examined and analytical expressions are given for the radiation efficiency for edge modes as a function of the angle $\varphi$ of the baffle, and also for the combined influence of a rotational spring compliance $\varepsilon$ and the angle of baffle, $\varphi$. These expressions for the radiation efficiency are given as functions of the 'angle of propagation', $\theta$, of the bending waves.

Due to the high complexity of these expressions, it does not seem practical to calculate the modal averages of these radiation efficiencies. Instead, it is suggested to use the derived analytical expressions for the modal-averaged radiation efficiency $\bar{\sigma}_{ss}$ as *base-line predictions* and to modify/correct these by a multiplication correction-factor $Q(\gamma)$, which accounts for the radiation effects of the actual edge constraints and the baffle angle if this is different from $\pi$. Expressed as a function of the 'global' wavenumber ratio $\gamma = k_0/k_b$ this correction-factor, $Q(\gamma)$, can be calculated numerically as [10]

$$Q(\gamma) = \frac{2}{\pi} \int_0^{\pi/2} \frac{\sigma_{\phi,\varepsilon}(\gamma, \theta)}{\bar{\sigma}_{ss}} \mathrm{d}\theta, \tag{16}$$

where $\sigma_{\varphi,\varepsilon}(\gamma, \theta)$ is the radiation efficiency for the type of baffle angle and edge modes in question.

The variations of the correction-factor $Q(\gamma)$ have been computed for three important practical cases of baffle angle, $\varphi = \pi/2, \pi, 3\pi/2$, with the edge-constraint compliance $\varepsilon$ as parameter; this is

expressed in a non-dimensional form by the product $k_0\varepsilon D$, where $D$ is the plate bending stiffness. Fig. 4 shows the computed results, which are based on the assumption that the boundary conditions and the baffle angles are identical at all four plate-edges. In addition, it has been assumed that $\sigma = 0$ in the corner mode range: $\alpha > 1 \wedge \beta > 1$. The results in Fig. 4 are seen to agree with the expected limiting values [7], that is

$$Q(\gamma) = 2 \quad \text{for } \varepsilon = 0 \wedge \ \varphi = \pi, \quad Q(\gamma) = \frac{\pi}{\varphi} \quad \text{for } \varepsilon \to \infty \wedge \gamma \ll 1. \tag{17, 18}$$

Eq. (17), for example, shows that the radiation from a clamped plate in a co-planar baffle is enhanced by a factor of two in comparison to the traditional base-line radiation $\bar{\sigma}_{ss}$ of the simply supported case. Moreover, from Fig. 4b it is seen that the radiation of a clamped plate radiating

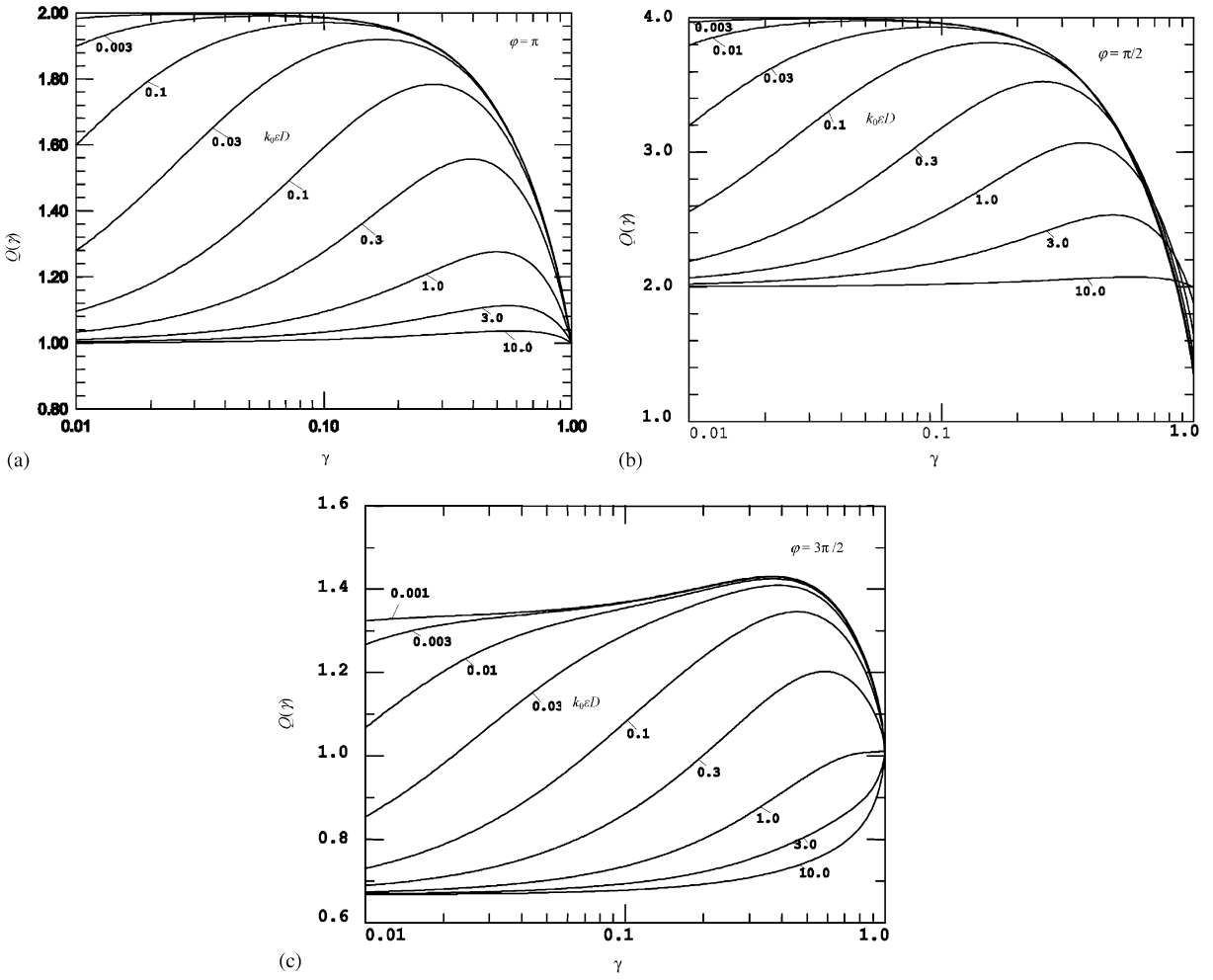


Fig. 4. Correction factor $Q(\gamma)$ as a function of wavenumber ratio $\gamma = k_0/k_b$ for an isotropic plate, with $k_0\varepsilon D$ as parameter. Baffle configurations: (a) co-planar baffle, $\varphi = \pi$; (b) rectangular duct-baffle, $\varphi = \pi/2$; and (c) duct-excluded free-space, $\varphi = 3\pi/2$.

into a rectangular room is expected to increase by a factor of *four* for $\gamma < 0.1$ in comparison to the traditional base-line radiation, $\bar{\sigma}_{ss}$.

Thus, for a given value of $\gamma = k_0/k_b$ and a specific value of $\varepsilon$, the product $k_0 \varepsilon D$ is calculated and the correction-factor $Q(\gamma)$ can be interpolated from Fig. 4. The modal-averaged radiation efficiency for the edge modes can then be calculated as

$$\bar{\sigma}(\gamma) = Q(\gamma)\bar{\sigma}_{ss}(\gamma) \quad \text{for } \gamma \leqslant 1. \tag{19}$$

Above the coincidence frequency (i.e., for $\gamma > 1$), the whole plate surface is radiating sound power and the influence of constrained edges and the angle of the baffle are negligible. If the boundary constraint conditions given by $\varepsilon$ and the angle $\varphi$ of the baffle are different for the various plate edges, then an average value of $Q(\gamma)$ can be estimated as shown in Ref. [10].

## 4. Predictions and experimental validation of sound radiation from a plate under the influence of baffle angle and edge constraints

In order to demonstrate and validate the influence of baffle angles and boundary constraint conditions, the radiation efficiency of an isotropic plate was predicted numerically and subsequently measured. This was done for a single test case of a rectangular aluminium-alloy plate for the three configurations of baffle angles studied in the previous section, that is, for $\varphi = \pi/2$, $\pi$ and $3\pi/2$. The practical implementation of these three baffle configurations is illustrated in Fig. 5.

### 4.1. Plate dimensions and experimental arrangement

The dimensions of the aluminium-alloy plate were $0.61 \times 0.37 \times 0.003$ m. The plate was bolted on to the end of a four-panel, welded box-frame that was made out of 3 mm steel plates. This assembly was then placed in the baffle fixture. The dimensions of the large plane baffle being used in the configuration shown in Fig. 5a was $1.9 \times 1.1$ m. This baffle was also employed in Fig. 5b in order to acoustically screen and hence minimize sound radiation contributions from the supporting box-frame. The open-ended, rectangular 'duct'-baffle used in Figs. 5b and c had a length of 0.8 m and a cross-section of $0.64 \times 0.40$ m. The small space between baffle and test-plate was sealed by elastic tape and soft rubber sealing-material that also served to isolate the baffle from the vibrating plate. The test arrangement was placed in a well-damped room with a reverberation time of 0.3 s and a volume of 295 $m^3$.

The aluminium plate was point-excited with random noise by a small electro-dynamic shaker. The spatial mean-square velocity of the plate was measured with a 2.5 g accelerometer by averaging the autospectra for 12 randomly chosen response positions. The velocity level at the plate junctions was also measured in order to ensure that the edge motion was negligible. In the frequency range from 80 to 1600 Hz it was found that the edge velocity level was from 30 to 20 dB lower than the velocity level of the plate vibration. The sound power radiated from the plate was determined by measuring the sound intensity over a control surface close to the plate; these sound intensity measurements were carried out both with 12 and 50 mm spacers to achieve the best possible accuracy in the examined frequency range. From these measurements the radiation

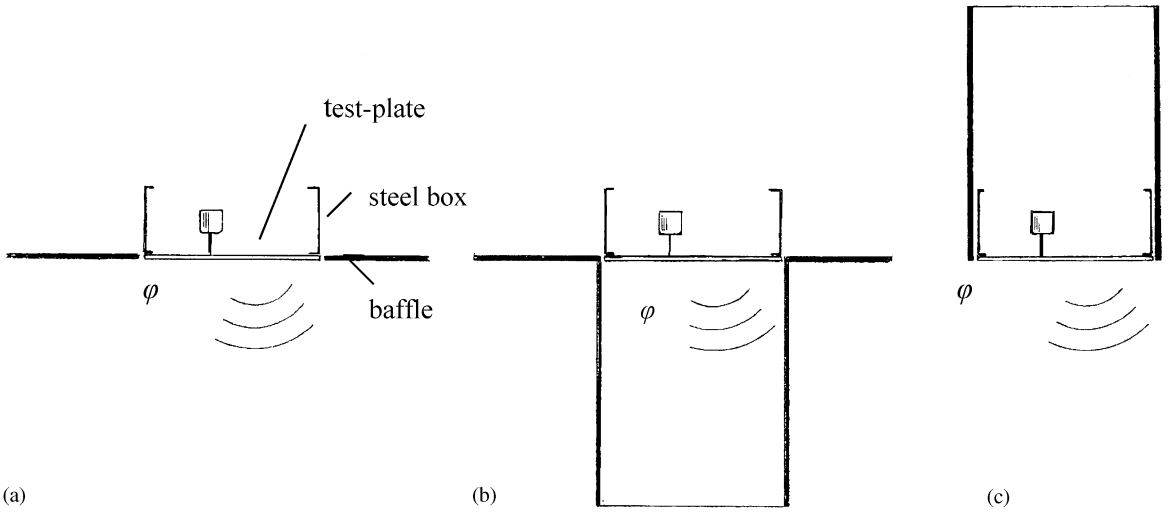


Fig. 5. Three baffle configurations for calculating and measuring plate radiation efficiencies. Baffle angle: (a) $\varphi = \pi$; (b) $\varphi = \pi/2$; and (c) $\varphi = 3\pi/2$.

efficiencies of the plate were calculated and the results were synthesized in $\frac{1}{3}$-octave bands. A dual-channel FFT-analyser was used as front-end in all measurements.

### 4.2. Determination of plate-edge constraints

In order to be able to predict the correction-factor $Q(\gamma)$ and hence the radiation efficiency $\bar{\sigma}$ it is necessary to know the apparent rotational spring compliance $\varepsilon$ that is used for describing the actual edge constraints at the plate boundary. As the edge constraints of the plate will control its resonance frequency, it is possible to estimate $\varepsilon$ from measurements of the plate's resonance frequencies and corresponding mode shapes of assumed mode numbers $(m, n)$. However, in the present case the estimation of the edge compliance $\varepsilon$ can only be done approximately, because the plate vibration cannot be separated from the vibration of the box-frame; the assembly vibrates as a whole, and vibration of the adjacent box-panels enforces different deformation shapes in the test-plate at the system's natural frequencies. Being part of a larger assembly which influences the deformation shape of the test-plate is of course a very realistic boundary environment for a plate. Alternatively, $\varepsilon$ could also be estimated from a FEM-analysis of the whole system. Fig. 6 shows the response-grid $(x_1, y_1, z_1)$ used for measuring the global mode shapes of the test-plate and adjacent plates of the supporting box-frame. The origin of this coordinate system is located at the off-centre driving point. The input mobility measured at this point was used for determining the system's resonance frequencies and associated damping loss factors, being found from their 3 dB-bandwidth in a polar- or Nyquist-diagram. Further, the global mode shapes were determined by using pure-tone excitation.

Two examples of such measured global mode shapes of the assembly are illustrated in Fig. 7 by projecting the modal deformations onto the plane of the paper. With respect to the aluminium test-plate, its deformation shape and boundary conditions for the identified mode $(m, n) = (1, 2)$

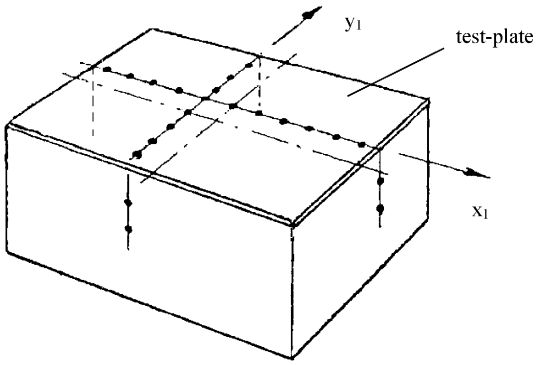


Fig. 6. Response-grid $(x_1, y_1, z_1)$ for measuring global mode shapes of test-plate and supporting box-structure. Origin of co-ordinate system is located at the off-centre driving point.

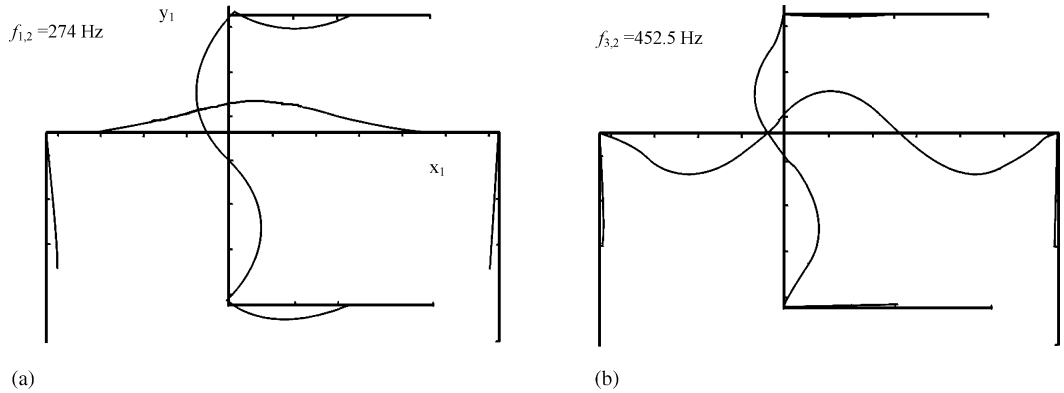


Fig. 7. Measured global mode shapes of test-plate and supporting box structure at (a) $f_{1,2} = 274$ Hz and (b) $f_{3,2} = 452.5$ Hz. Major horizontal and major vertical lines are measurement-grid in $x_1$ and $y_1$ and mode deformation of test-plate. Deformation of the supporting box panels is also shown.

are seen to closely resemble a plate mode with clamped-like, $y$-going edges for $m = 1$, and apparently simply-supported, $x$-going edges for $n = 2$. Similarly, the deformation shape of mode (3,2) is seen to resemble a virtually fully clamped test-plate.

A close inspection of the mode shape at the plate edges in Fig. 7a reveals that in addition to the rotation there is also a very small displacement of the $x$-going junctions, which is caused by a rigid-body rocking motion of the box. The influence of such a moving support is not accounted for in Leppington's model of a simply supported plate edge with a rotational line spring. However, in the present case the dipole-type sound radiation from the rocking motion of the box with $\sigma(274) \sim 0.5$ can be neglected, as its radiation contribution is only 3% of that caused by the elastic plate mode with $\sigma_{2,1} = 0.02$. This results from the velocity amplitude of the rocking motion being only $\frac{1}{30}$ of the plate amplitude.

Table 1 shows the measured resonance frequencies and associated mode numbers, the predicted natural frequencies for simply supported and clamped cases, measured damping loss factors $\eta$, and the resulting estimated product of the spring compliance and bending stiffness, $\varepsilon D$. The given

Table 1
Measured mode numbers and resonance frequencies, predicted natural frequencies for simply supported/clamped conditions, measured damping loss factors and estimated product of $\varepsilon D$

| Mode $(m,n)$ | $f_{m,n}$ (Hz) | $f_{m,n}$ (simply s./clamped) (Hz) | $\eta$ | $\varepsilon D$ |
|---|---|---|---|---|
| (1,1) | 118.5 | 75/144 | 0.016 | 0.0268 |
| (2,1) | 170.5 | 135/209 | 0.014 | 0.0365 |
| (2,1) | 204.0 | 135/209 | 0.015 | 0.0025 |
| (3,1) | 270.0 | 235/321 | 0.008 | 0.0363 |
| (1,2) | 274.0 | 238/362 | 0.008 | 0.0773 |
| (3,1) | 291.0 | 235/321 | 0.010 | 0.0134 |
| (1,2) | 301.5 | 238/362 | 0.008 | 0.0300 |
| (2,2) | 352.0 | 299/424 | 0.005 | 0.0365 |
| (4,1) | 423.0 | 376/478 | 0.009 | 0.0222 |
| (3,2) | 452.5 | 399/528 | 0.004 | 0.0319 |

mode numbers apply for the deformation shape of the test-plate only. The resonance frequencies at 170.5 and at 204 Hz will, for the assembly, have different mode shapes but the deformation shapes of the test-plate are very similar for these two cases. Most of the measured resonance frequencies are seen to be close to a mean value of the theoretical values of the natural frequencies for the simply supported and clamped cases.

It is recalled that the estimated spring compliance $\varepsilon$ corresponds to a simply supported plate with a rotational edge constraint given by $\varepsilon D$ that has the mode numbers $(m,n)$ and natural frequency, $f_{m,n}$. The use of a least-squares-fit to the measured results gives the frequency dependency of the product $\varepsilon D$ as

$$\varepsilon D = 0.0285 + 0.989 \times 10^{-5} f. \tag{20}$$

This, together with the wavenumber ratio $\gamma$ and acoustic wavenumber $k_0$ permits the correction-factor $Q(\gamma)$ to be read from Fig. 4.

### 4.3. Predicted and measured radiation efficiencies

The final numerical predictions of the plate radiation efficiencies for the three baffle angles are shown in Fig. 8 together with the measured results. Here, the predicted modal-averaged radiation efficiency $\bar{\sigma}$ includes corrections for the influence of both baffle angle and boundary constraint conditions, given by Eq. (20). Thus, since $\bar{\sigma} = Q(\gamma)\bar{\sigma}_{ss}$, the predicted overall influence of the correction-factor $Q(\gamma)$ is seen by comparison with the 'base-line' prediction $\bar{\sigma}_{ss}$, which is also included in Fig. 8.

Results for the classical case of a plane baffle, $\varphi = \pi$, are shown in Fig. 8a. It is seen that the predicted increase in radiation efficiency due to the edge constraint is reasonably well validated by the measurements, although some discrepancies occur at the lower frequencies. This is possibly caused by the small number of radiating plate modes, see Table 1. With a plate modal density of $n(f) = 0.024$ this corresponds on average to a single mode in the $\frac{1}{3}$-octave band of 200 Hz and three modes in the 500 Hz band.

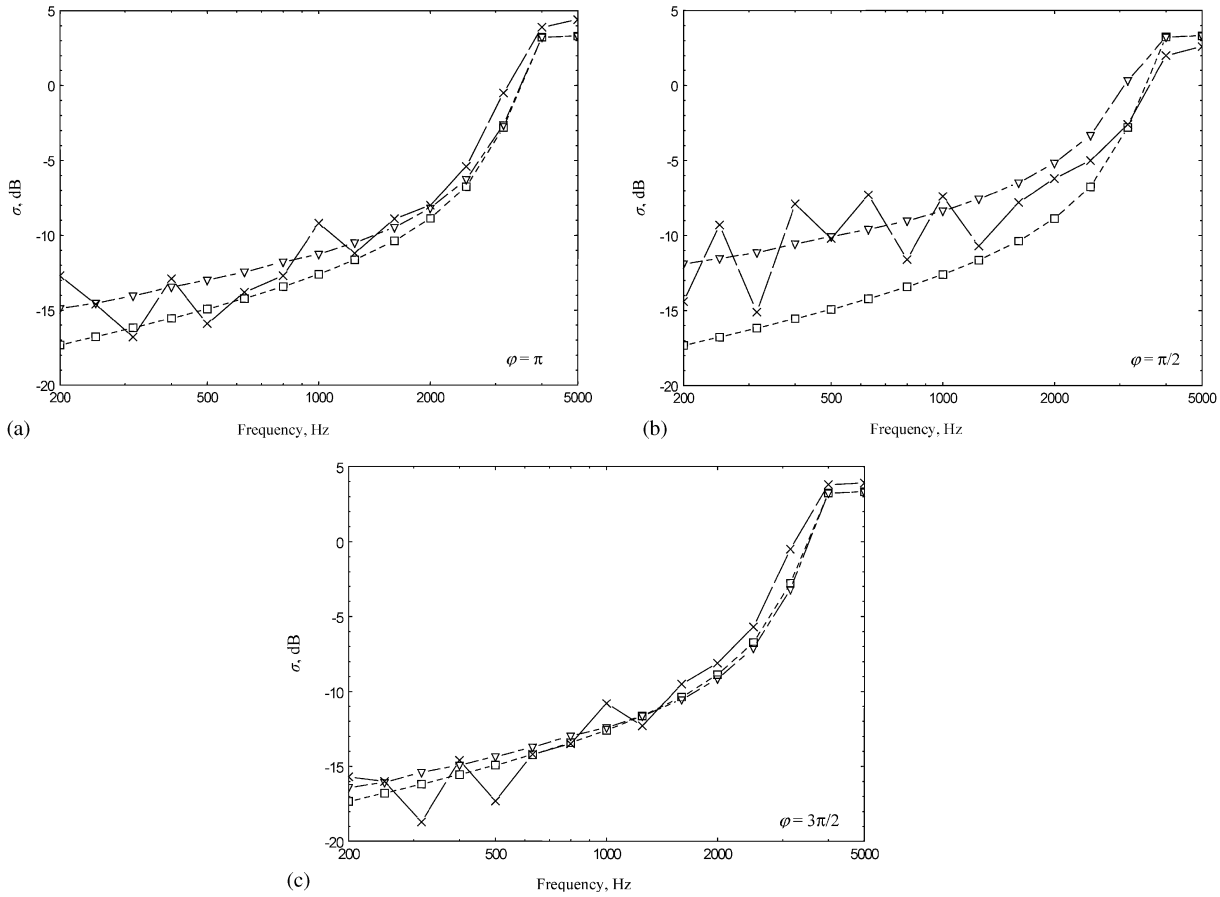


Fig. 8. Modal-averaged radiation efficiencies of an isotropic, rectangular plate that is bounded by different baffle configurations: ∇---∇, predicted results for $10\log\bar{\sigma}$; ×---×, measured results for $10\log\bar{\sigma}$; □---□, uncorrected base-line prediction for $10\log\bar{\sigma}_{ss}$. Baffle angle: (a) $\varphi=\pi$; (b) $\varphi=\pi/2$; and (c) $\varphi=3\pi/2$.

For a baffle angle of $\varphi=\pi/2$, the increase in sound radiation due to the baffle alone is expected to be 3 dB, cf. Eq. (18). This radiation is further enhanced by the contribution due to the constrained edges. Fig. 8b shows that this trend is generally confirmed, although the predicted results at the higher frequencies exceed the measured values by about 2 dB. Moreover, as the predicted results have been derived for one-sided radiation into three-dimensional free space, they are in principle not valid below the cut-off frequency (506 Hz) of the rectangular duct-baffle section, which has a cross-sectional opening of $0.64\times0.40$ m. However, on average the predicted results at low frequencies are seen to agree reasonably well with the measured values.

Finally, Fig. 8c shows the results for a baffle angle of $\varphi=3\pi/2$. In this case a slight radiation *decrease* of 1.8 dB is expected due to the baffle alone, cf. Eq. (18), in addition to an *increase* due to the edge constraint. The combined influence of these two factors is a small enhancement of the radiation at low frequencies, while at higher frequencies a small decrease is predicted. This specific

spectral trend is not found in the measured results, although the overall agreement with the prediction is seen to be fairly good. Still, some of the bias-effect may be overcome by making a relative comparison of the measured results only. So, if the measurements for this condition is compared directly with the measurements for the plane-baffle-case (Fig. 8a), it is seen that the radiation in the present $3\pi/2$-case on average is lower by 1.6 dB in the frequency range up till 1600 Hz, and this is close to the predicted effect.

## 5. Discussions and conclusion

The non-dimensional $(\alpha, \beta)$-representation of the radiation efficiency, as derived by Leppington et al., permits calculation of the modal-averaged radiation efficiency for a given type of plate. These results have been employed here to calculate modal-averaged correction-factors for isotropic plates and modal-averaged radiation efficiencies for orthotropic plates. The correction-factor allows the base-line radiation efficiency to be corrected for the influence of the angle of wedge-shaped baffles and the influence of the boundary conditions (edge constraint). The calculations show that the radiation may be enhanced by a factor of four for a clamped plate radiating into a rectangular room in comparison with the well-known base-line prediction for a simply supported plate in a co-planar baffle. Predicted radiation efficiencies for a vibrating test-plate with realistic boundary conditions otherwise set in three types of practical baffle configurations have been compared with measured values with good agreement. The examined cases of baffle configurations are of practical importance in the prediction of sound radiation into confined spaces like cockpits, cabins and rooms, and for the prediction of out-wards sound radiation from closed structures such as cabinets, machine-type panels and the like.

## References

[1] R.H. Lyon, R.G. DeJong, *Theory and Application of Statistical Energy Analysis*, Butterworth-Heinemann, Boston, 1995.
[2] G. Maidanik, Response of ribbed panels to reverberant acoustic fields, *Journal of the Acoustical Society of America* 34 (6) (1962) 809–826.
[3] F.G. Leppington, E.G. Broadbent, K.H. Heron, The acoustic radiation efficiency of rectangular panels, *Proceedings of the Royal Society of London, Series A* 382 (1982) 245–271.
[4] K.H. Heron, Acoustic radiation from honeycomb sandwich plates, *Fifth European Rotorcraft and Powered Lift Aircraft Forum*, Amsterdam, 1979, paper 65, pp. 1–12.
[5] F.J. Fahy, *Sound and Structural Vibration, Radiation, Transmission and Response*, Academic Press, London, 1987.
[6] F.G. Leppington, E.G. Broadbent, K.H. Heron, Acoustic radiation from rectangular panels with constrained edges, *Proceedings of the Royal Society of London, Series A* 393 (1984) 67–84.
[7] F.G. Leppington, Acoustic radiation into a wedge-shaped region: application to the free plate problem, *Proceedings of the Royal Society of London* 452 (1996) 1745–1764.
[8] W. Soedel, *Vibrations of Shells and Plates*, Marcel Dekker, New York, 1993.
[9] R.S. Langley, Elastic wave transmission coefficients and coupling loss factors for structural junctions between curved panels, *Journal of Sound and Vibration* 169 (3) (1994) 297–317.
[10] ESDU Data Item 00002, Radiation efficiencies of isotropic plates, ESDU International plc, London, UK, 2000.